Shielding Effectiveness Estimation of a Metallic Enclosure with an Off-center Aperture for Obliquely Incident and Arbitrary Polarized Plane Wave

Dan Shi, Na Lv, and Yougang Gao

Department of Electronic Engineering
Beijing University of Posts and Telecommunications, Beijing, 100000, China
shidan@buptemc.com

Abstract ─ A circuit model for the shielding effectiveness (SE) estimation of a metallic enclosure is proposed, whose off-center aperture is irradiated by the obliquely incident and arbitrary polarized plane wave. This new model has advantages in the following aspects. First, it can deal with the arbitrary angular and polarized incident wave other than the normal incident wave. The incident wave angle and polarization direction are considered in the proposed analytical formulas. Second, higher-order modes such as TEmn and TMmn are included to enable the model to be applicable in higher frequencies. Third, the impedance of the enclosure wall is considered rather than the perfect conductor assumption used in the published literatures, which removes the deficiency that the aperture impedance is zero when the length of the aperture is equal to an integral number of the wavelengths. The influences on the SE from different parameters such as the incident wave angle, the polarization direction as well as the enclosure wall thickness are investigated. Finally, the accuracy of the proposed model is validated by measurements, simulations and comparisons with other literatures. The proposed method is particularly useful for the shielding enclosure design in the electronic manufacturing industry.

Index Terms ─ Circuit model, higher-order modes, obliquely incident, rectangular enclosure, shielding effectiveness.

I. INTRODUCTION

The shielding enclosure has been widely used in the electronic system to reduce the emissions or improve the immunity. The performance of a shielding enclosure is assessed by its shielding effectiveness (SE), defined as the ratio of field strengths in the presence and absence of the enclosure. However, the SE is often deteriorated by the apertures or slots for the input and output connections, heat dissipation, control and ventilation. Thus, in the published literatures, numerous approaches have been presented for calculating the SE of the shielding enclosures with apertures and slots, mainly including numerical methods and analytical formulations. The numerical methods such as the transmission-line modeling method [1], the finite-difference time-domain method [2], the method of moments [3], [4], the finite element method [5], and the hybrid methods [6] can model and calculate the complex structures, but it is difficult for designers to use them to investigate the effect of various parameters. In addition, they are computationally intensive when the thickness of the enclosure wall is much smaller than the enclosure dimension size. Meanwhile, most analytical formulations are based on the equivalent circuit method proposed by Robinson [7], where the aperture and the enclosure are assumed to be the length of a coplanar strip transmission line, and a rectangular waveguide ended with a short circuit. The model is limited to the center aperture and the TE10 mode. The method was extended in [8] to include the effects of loading the enclosure with some printed circuit board structures. The enclosure with apertures on multiple sides considering the oblique incidence and polarization was studied in [9]. [10] applied the concept of quasi-stationary admittance of diaphragms inside a rectangular waveguide and their equivalent circuits to investigate the SE of an enclosure with an aperture. The SE of the rectangular enclosure with an off-center aperture was analyzed in [11]. However, some important design parameters, such as the incident wave angle and polarization direction, have not been thoroughly investigated in the published literatures.

In this paper, a more general approach is proposed to evaluate the SE of a rectangular enclosure with an off-center aperture. The incident wave angle and the polarization direction are included in the analytical formulation. The proposed method can handle an arbitrary locational aperture in the higher frequencies. Moreover, the thickness of the enclosure wall is considered, which removes the limitation that the SE is erroneously predicted to be infinite when the length of the aperture corresponds to an integer multiple of wavelength for the traditional circuit models.

II. PROPOSED MODEL AND FORMULATION

The geometry of the enclosure with an aperture is shown in Fig. 1. The thickness of the enclosure wall is t. A plane wave as an excitation source has its incident angle θ and polarization angle φ.
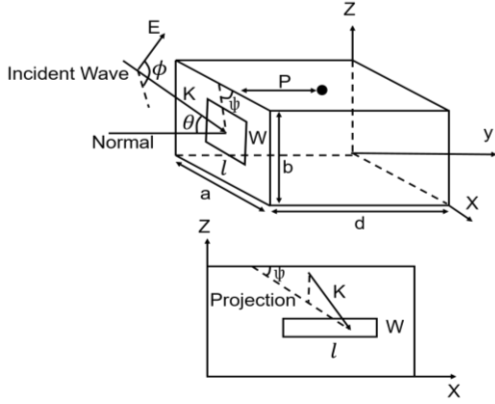

Fig. 1. The obliquely incident wave and the enclosure with an aperture.

Figure 2 shows the obliquely incident wave in the front face. The electric field E is decomposed into the x-component, the y-component and the z-component fields by the vector analysis. The normal vector of the front face of the enclosure is $\mathbf{n}$, same as the direction of the y-axis. The propagation vector of the incident wave is named as $\mathbf{k}$ vector. The incident angle θ is defined as the angle between the propagation vector $\mathbf{k}$ and the normal vector $\mathbf{n}$, and these two vectors determine the incident plane. The angle between the E field and the incident plane is defined as the polarization angle φ. The angle between the projection of the propagation vector $\mathbf{k}$ in the X-Z plane and the x-axis is defined as ψ. The decompositions of the E field are as follows:

x-component: $-E\cos\varphi\cos\theta\cos\psi + E\sin\varphi\sin\psi$,

y-component: $E\cos\varphi\sin\theta$,

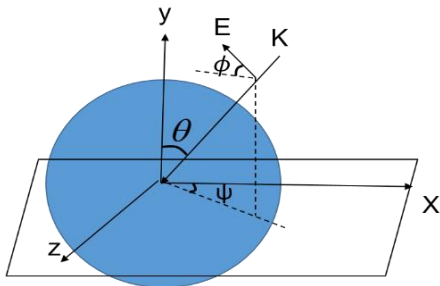z-component: $-E\cos\varphi\cos\theta\sin\psi - E\sin\varphi\cos\psi$.

Fig. 2. The vector analysis of an obliquely incident wave.

For the x-component and the z-component of the

electric field E, the wave propagates along the y-axis into the enclosure. However, for the y-component, the wave propagates along the z-axis and reflects back and forth, which has small contributions to the field in the enclosure and is ignored in the calculation.

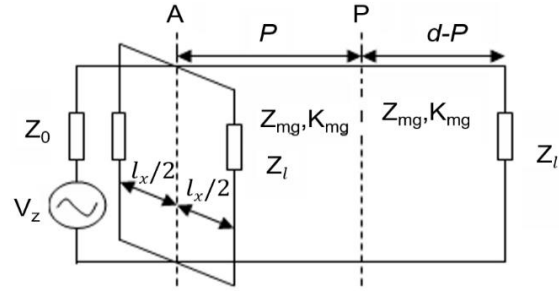For the z-component, the equivalent circuit model is shown as Fig. 3.

Fig. 3. The equivalent circuit of an enclosure with an aperture.

The aperture is represented as a coplanar strip transmission line with the length of the aperture in the x-direction. Owing to the loss of the enclosure wall, the transmission line is loaded with the impedance Z_l at each end. Based on Gupta's theory [12], the characteristic impedance of the transmission line is:

$$Z_{os1} = 120\pi^2 \left[\ln\left(2\frac{1+\sqrt[4]{1-(w_{e1}/b)^2}}{1-\sqrt[4]{1-(w_{e1}/b)^2}} \right) \right]^{-1}. \quad (1)$$

The effective width w_{e1} is:

$$w_{e1} = w - \frac{5t}{4\pi}\left(1+\ln\frac{4\pi w}{t}\right), \quad (2)$$

where t is the thickness of the enclosure wall and w is the width of the aperture in the z-direction.

A coupling co-efficient C_m, obtained by enforcing the field continuity at the aperture such that the total modal fields at the aperture are consistent with the aperture field, is introduced to account for the coupling between the aperture and the enclosure:

$$C_m = \int_{x_0}^{x_0+l}\int_{z_0}^{z_0+w}\cos\left(\frac{n\pi z}{b}\right)\cos\left(\frac{n(z-z_0)\pi}{w}\right)\sin\left(\frac{\pi m x}{a}\right)\sin\left(\frac{m\pi(x-x_0)}{l}\right)dxdz \bigg/ XZ, \quad (3)$$

where x_0 and z_0 are the coordinates of the first edge of the aperture, X and Z are the coordinates of the aperture center. The load impedance Z_l at the ends of the transmission line is transformed through a distance $l/2$ to the center to calculate the aperture impedance Z_{ap1}:

$$Z_{ap1} = \frac{1}{2}C_m Z_{os1} \frac{Z_l + jZ_{os1}\tan(k_0 l/2)}{Z_{os1} + jZ_l\tan(k_0 l/2)}, \quad (4)$$

where $Z_l = (1+j)\sqrt{\pi f\mu_1/\sigma}$, μ_1 and σ are the permeability and conductivity of the enclosure.

By Thevenin's theorem, the equivalent source voltage V_{1z} and source impedance Z_{1z} are determined by:

$$V_{1z} = V_z Z_{ap1} / (Z_0 + Z_{ap1}), \qquad (5)$$

$$Z_{1z} = Z_0 Z_{ap1} / (Z_0 + Z_{ap1}), \qquad (6)$$

where source voltage V_z is $-V_0 (\cos\phi\cos\theta\sin\psi + \sin\phi\cos\psi)$.

The equivalent voltage V_{2z} and the source impedance Z_{2z} are obtained by transforming V_{1z} and Z_{1z} to the test point P:

$$V_{2z} = V_{1z} / (\cos(k_{mg}p) + j(Z_{1z} / Z_{mg})\sin(k_{mg}p)), \qquad (7)$$

$$Z_{2z} = Z_{mg} \frac{Z_{1z} + jZ_{mg}\tan(k_{mg}p)}{Z_{mg} + jZ_{1z}\tan(k_{mg}p)}. \qquad (8)$$

For the TE$_{mn}$ propagation mode, the waveguide modal impedance and the propagation constant are:

$$Z_{mg} = Z / \sqrt{1 - (m\lambda/2a)^2 - (n\lambda/2b)^2}, \qquad (9)$$

$$k_{mg} = k\sqrt{1 - (m\lambda/2a)^2 - (n\lambda/2b)^2}. \qquad (10)$$

For the TM$_{mn}$ propagation mode, the waveguide modal impedance and the propagation constant are:

$$Z_{mg} = Z\sqrt{1 - (m\lambda/2a)^2 - (n\lambda/2b)^2}, \qquad (11)$$

$$k_{mg} = k\sqrt{1 - (m\lambda/2a)^2 - (n\lambda/2b)^2}, \qquad (12)$$

where $k = 2\pi / \lambda, Z = \sqrt{\mu/\varepsilon}$, μ and ε are the permeability and the dielectric permittivity of the material in the enclosure, and m and n are the modes of TE and TM wave.

Transform the load impedance Z_l at the end of the waveguide to the test point P, and the load impedance Z_3 is represented as:

$$Z_3 = Z_{mg} \frac{Z_l + jZ_{mg}\tan k_{mg}(d - p)}{Z_{mg} + jZ_l \tan k_{mg}(d - p)}. \qquad (13)$$

Accordingly, the voltage at the test point is equal to $V_{pm1} = V_{2z}Z_3 / (Z_{2z} + Z_3)$. For the multi-modes in the enclosure, the total voltage at the test point is given by:

$$V_{tpml} = \sum V_{pm1}. \qquad (14)$$

For the x-component of the E field, the equivalent circuit model is similar to Fig. 3, simply replacing the source voltage V_z and coplanar transmission line l with V_x and w respectively. The source voltage V_x is equal to $V_0(\sin\phi\sin\psi - \cos\phi\cos\theta\cos\psi)$.

The characteristic impedance of the coplanar transmission line is:

$$Z_{os2} = 120\pi^2 \left[\ln\left(2(1 + \sqrt[4]{1 - (w_{e2}/a)^2}) / (1 - \sqrt[4]{1 - (w_{e2}/a)^2}) \right) \right]. \qquad (15)$$

The effective width w_{e2} is:

$$w_{e2} = l - \frac{5t}{4\pi}\left(1 + \ln\frac{4\pi l}{t}\right). \qquad (16)$$

The aperture impedance Z_{ap2} can be calculated by transforming the load impedance Z_l at the ends of the aperture through a distance $w/2$ to the center:

$$Z_{ap2} = \frac{1}{2} C_m Z_{os2} \frac{Z_l + jZ_{os2}\tan(k_0 w/2)}{Z_{os2} + jZ_l \tan(k_0 w/2)}. \qquad (17)$$

Similarly, the voltage V_{pm2} at the test point P from the effect of the x-component of the E field can be obtained by replacing the source voltage V_z and the aperture impedance Z_{ap1} with V_x and Z_{ap2} from (5)-(14). The total voltage at the test point for the multi-modes is:

$$V_{tpm2} = \sum V_{pm2}. \qquad (18)$$

Finally, the total voltages at the observing point P is given by the combination of the contributions from the x-component and z-component:

$$V_{ptotal} = \sqrt{V_{tpm1}^2 + V_{tpm2}^2}. \qquad (19)$$

In the absence of the enclosure, the load impedance at P is simply Z_0 and the voltage V_p is equal to $V_0/2$. Therefore, the electric shielding effectiveness is written as:

$$S_E = 20\log_{10}|V_p/V_{ptotal}| = 20\log_{10}|V_0/2V_{ptotal}|. \qquad (20)$$

III. NUMERICAL RESLULTS AND MEASUREMENT

The enclosure for testing is with the dimensions of 30 cm × 40 cm × 20 cm, and an aperture with the dimensions of 5 cm × 1cm is located at the off-center position in the front face. The enclosure is filled with air. The coordinates of the aperture center are X = 14.5 cm and Z = 10 cm. As the operating frequency of the electronic equipment gets higher and higher, many higher modes propagate in the enclosure other than only the dominant mode. The cut-off frequency of each mode is listed in the Table 1 according to (21). Thus, the modes TE$_{10}$, TE$_{01}$, TE$_{20}$, TE$_{02}$, TE$_{11}$, TE$_{12}$, TE$_{21}$, TE$_{22}$, TM$_{11}$, TM$_{21}$, and TM$_{12}$ should be considered if the operating frequency is between the frequency band 1 GHz ~ 1.26 GHz.

$$f_c = \sqrt{(m/a)^2 + (n/b)^2} / 2\sqrt{\mu\varepsilon}, , \qquad (21)$$

where m and n are the modes of TE and TM wave.

Table 1: Cut-off frequency (MHz) for modes in the enclosure

n \ m	0	1	2
0	-	500	1000
1	375	625	1070
2	750	900	1250

According to the cut-off frequencies of different modes and the incident wave frequency, the modes considered in the analytical formulas are determined. Thus, the SE of the enclosure with an aperture can be

calculated with the proposed formulas. To validate the results, some measurements were carried out in a fully anechoic chamber (FRANKONIA). A network analyzer (E8363B, Agilent) connected via an amplifier to a log-periodic antenna (HL 562, R&S) was used to generate the source. The SE measurements were made by a small dipole antenna in the enclosure connected to the port 2 of the network analyzer. The SE was determined by the difference between the S21 for the shielded and unshielded cases.

Three cases of the normal incidence and the oblique incidence are investigated. First, the normal incident case for the vertical polarization is analyzed, where $\theta = 0$, $\phi = 90^0$ and $\psi = 0$.

Figure 4 represents the SE of the test point (14.5 cm $\times$ 20 cm $\times$ 10 cm). In the graph, the solid line shows the calculated results using the proposed model and the dotted line shows the results from the measurement.
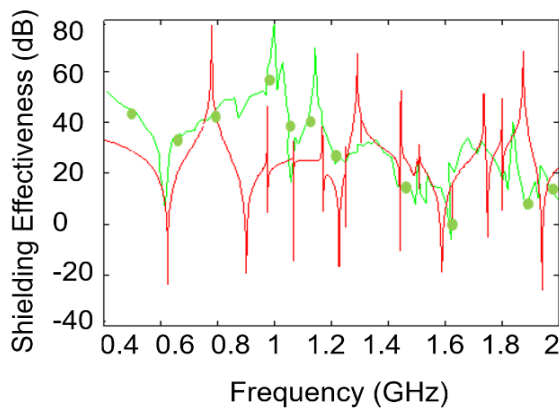

Fig. 4. The electric SE for the normal incident case. Solid line: our model. Dotted line: measurement.

Figure 4 shows that the SE deteriorates significately at those resonant frequencies. The proposed method can predict the multiple resonant points accurately. The resonant frequencies of different modes in the fabricated enclosure are given by the theoretical formula:

$$f = \frac{1}{2\sqrt{\mu\varepsilon}} \sqrt{\left(\frac{m}{a}\right)^2 + \left(\frac{n}{b}\right)^2 + \left(\frac{l}{d}\right)^2}. \qquad (22)$$

The SE obtained by the proposed methods decreases dramatically at 0.625 GHz, 0.9 GHz, 1.07 GHz, 1.25 GHz, 1.458 GHz, 1.58 GHz, 1.8 GHz, and 1.95 GHz, which are same as the resonant frequencies of modes TM_{110}, TE_{101}/TM_{120}, TM_{210}, TM_{220}, TE_{221}/TM_{221}, TE_{102}, TE_{202}, TE_{222}/TM_{222}, respectively. From Fig. 4 it is easy to find that the calculated results of the proposed model and the measured results are consistent in trend, especilaly at high frequencies. Therefore, higher-order modes should be included in the analytical formulas to get 0the

reasonable results in high frequencies.

Another case for the obliquely incident wave with $\theta = 60^o$, $\varphi = 30^o$, $\psi = 30^o$ is investigated. The SE of the enclosure from the proposed method and the measurement is displayed in Fig. 5.
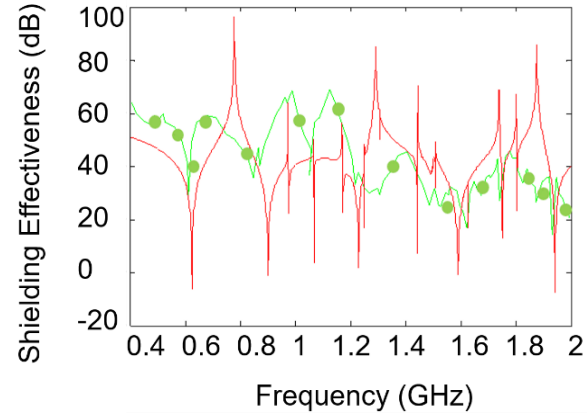

Fig. 5. The electric SE for the obliquely incident case. Solid line: our model. Dotted line: measurement.

The SE results for the obliquely incident wave with $\theta = 45^o$, $\varphi = 60^o$, $\psi = 45^o$ are displayed in Fig. 6, and the comparisons with the CST simulations are also included. It can be found that many resonances happened at high frequencies, so multimode analytical method should be applied instead of TE_{10} mode analysis.
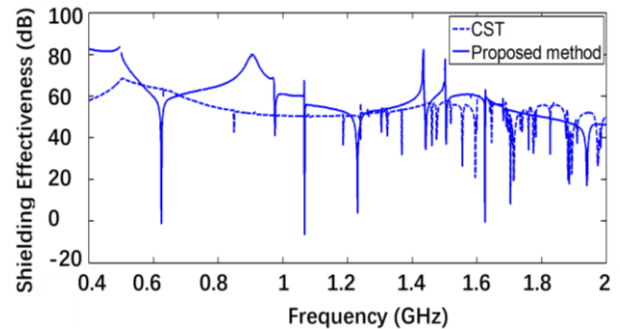

Fig. 6. The electric SE for obliquely incident case. Solid line: our model. Dotted line: CST simulation.

Some comparisons between the proposed method and other published literatures are also made. Table 2 shows the comparisons among the proposed method, the results from [11], and the results from the HFSS simulation. We can see that the results obtained with the proposed method are more consistent with the simulation results with HFSS than [11]. The excitation frequency is 700 MHz.

Table 2: Comparisons with other methods

Incident Angle	SE from the Proposed Method (dB)	SE from HFSS (dB)	SE from [11] (dB)
0°	20.54	14.03	-12.85
10°	20.67	14.78	-12.72
20°	21.08	15.88	-12.28
30°	21.79	17.3	-11.22
40°	22.85	23.74	-9.86
50°	24.38	26.7	-7.58
60°	26.56	26.94	-4.37
70°	29.85	28.34	-0.41
80°	35.73	28.71	6.63
90°	80.33	68.08	22.55

IV. DISCUSSION

Some parameters affecting the SE are studied in this part. The dimensions of the enclosure and the aperture are same as those in the part III.

A. SE varies with incident angle

The incident wave frequency is 1.1 GHz, and the polarization angle φ is 30°. The propagation vector of the incident wave is located at the X - Y plane, and the incident angle θ varies from 0 to 90°, leading to $\psi = 0$. Figure 7 demonstrates that the SE is the worst for the normal incident wave, and the SE increases with the incident angle until it reaches the maximum when the incident wave propagates along the long side of the aperture.
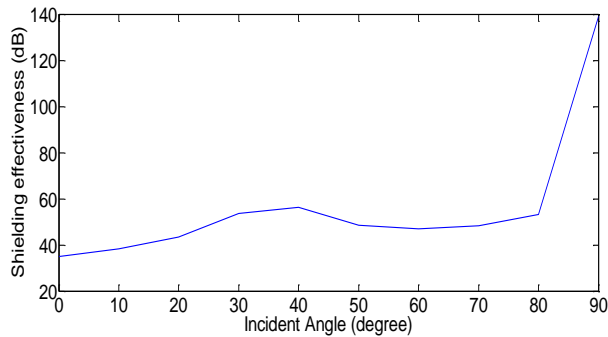

Fig. 7. The electric SE vs. the incident angle.

B. SE varies with the polarization angle

The incident angle θ in the X - Y plane is 30° and ψ is 45°. The polarization angle φ varies from 0 to 90°. Figure 8 shows that the SE is the worst when the polarization angle is 90°, in which case the *E*-field is perpendicular to the long side of the aperture. On the other hand, the SE reaches the maximum when the polarization angle φ is equal to 45° since the equivalent source is determined by the $\sin\varphi$ and $\cos\varphi$ simultaneously.
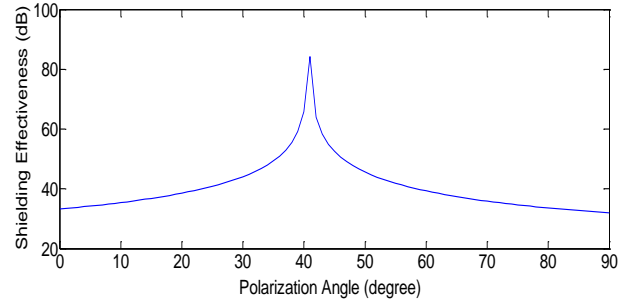

Fig. 8. The electric SE vs. the polarization angle.

C. SE varies with the enclosure wall thickness

The enclosure wall thickness, whose influence is explored, varies from 1 mm to 5 mm. The incident wave parameters are as: $\theta = 60°$, $\varphi = 30°$, $\psi = 30°$.

From Fig. 9, we can see that the SE increases with the enclosure wall thickness.
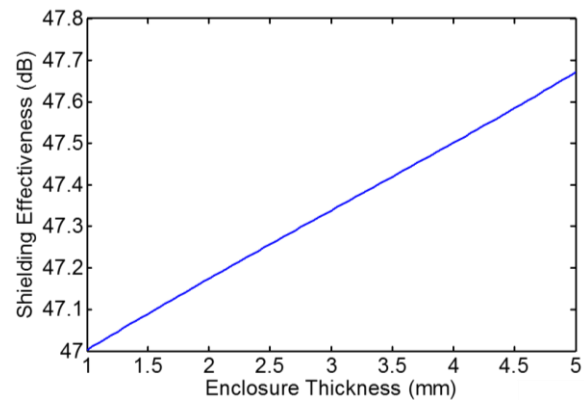

Fig. 9. The electric SE vs. the enclosure wall thickness.

V. CONCLUSION

The proposed model can calculate the SE of the rectangular enclosure with the off-center aperture fast and accurately. The oblique incidence and polarization are cogitated, and higher-order modes are included to enable the model to be applicable in higher frequencies. Therefore, the proposed analytical formulation is very useful for the practical design of the shielded enclosures in the electronic manufacturing industry.

ACKNOWLEDGMENT

REFERENCES

[1] B. L. Nie, P. A. Du, Y. T. Yu, and Z. Shi, "Study of the shielding properties of enclosures with apertures at higher frequencies using the transmission line modeling method," *IEEE Trans. Electromagn. Compat.*, vol. 53, no. 1, pp. 73-81,

Feb. 2011.

[2] C. Q. Jiao, L. Li, X. Cui, and H. Q. Li, "Subcell FDTD analysis of shielding effectiveness of a thin-walled enclosure with an aperture," *IEEE Transactions on Magnetics*, vol. 42, no. 4, 2006.

[3] R. Araneo and G. Lovat, "Fast MoM analysis of the shielding effectiveness of rectangular enclosures with apertures, metal plates, and conducting objects," *IEEE Trans. Electromagn. Compat.*, vol. 51, no. 2, pp. 274-283, May 2009.

[4] R. Araneo and G. Lovat, "Analysis of the shielding effectiveness of metallic enclosure excited by internal source through an efficient method of moment approach," *ACES Journal*, vol. 25, no. 7, pp. 600-611, July 2010.

[5] W. Abdelli, X. Mininger, L. Pichon, and H. Trabelsi, "Impact of composite materials on the shielding effectiveness of enclosure," *ACES Journal*, vol. 27, no. 4, pp. 369-375, Apr. 2012.

[6] C. Feng and Z. Shen, "A hybrid FD–MoM technique for predicting shielding effectiveness of metallic enclosures with apertures," *IEEE Trans. Electromagn. Compat.*, vol. 47, no. 3, pp. 456-462, Aug. 2005.

[7] M. P. Robinson, T. M. Benson, C. Christopoulos, J. F. Dawson, M. D. Ganley, A. C. Marvin, S. J. Porter, and D. W. P. Thomas, "Analytical formulation for the shielding effectiveness of enclosures with apertures," *IEEE Trans. Electromagn. Compat.*, vol. 40, no. 3, pp. 240-247, Aug. 1998.

[8] D. W. P. Thomas, A. C. Denton, T. Konefal, T. Benson, C. Christopoulos, J. F. Dawson, A. Marvin, S. J. Porter, and P. Sewell, "Model of the electromagnetic fields inside a cuboidal enclosure populated with conducting planes or printed circuit boards," *IEEE Trans. Electromagn. Compat.*, vol. 43, no. 2, pp. 161-169, May 2001.

[9] J. J. Shim, D. G. Kam, J. H. Kwon, and J. H. Kim, "Circuital modeling and measurement of shielding effectiveness against oblique incident plane wave on apertures in multiple sides of rectangular enclosure," *IEEE Trans. Electromagn. Compat.*, vol. 52, no. 3, pp. 566-577, Aug. 2010.

[10] B. l. N. and P. A. D., "An efficient and reliable circuit model for the shielding effectiveness prediction of an enclosure with an aperture," *IEEE Trans. Electromagn. Compat.*, vol. 57, no. 3, pp. 357-364, June 2015.

[11] C. C. Wang, C. Q. Zhu, X. Zhou, and Z. F. Gu, "Calculation and analysis of shielding effectiveness of the rectangular enclosure with aperture," *ACES Journal*, vol. 28, no. 6, pp. 535-544, June 2013.

[12] K. C. Gupta, R. Garg, and I. J. Bahi, *Microstip Lines and Slotlines*. Artech House, Norwood, MA, 1979.

Dan Shi received Ph.D. degree in Electronic Engineering from Beijing University of Posts & Telecommunications, Beijing, China in 2008. She has been working in Beijing University of Posts & Telecommunications. Her interests include electromagnetic compatibility, electromagnetic environment and electromagnetic computation. She has published more than 100 papers. She is the Chair of IEEE EMC Beijing chapter, Vice Chair of URSI E Commission in China, General Secretary of EMC Section of China Institute of Electronics.

Na Lv received her Bachelor degree in Communication Engineering from Beijing University of Posts and Telecommunications in Beijing, China in 2015. Now she is studying for Master degree in Beijing Univer-sity of Posts and Telecommunica-tions in Beijing, China. Her research interests include electromagnetic compatibility and electromagnetic environment.

Yougang Gao received his B.S. degree in Electrical Engineering from National Wuhan University, China in 1950. He was a Visiting Scholar in Moscow Technical University of Communication and Information in Russia from 1957 to 1959. He is now a Professor in Beijing University of Posts and Telecommunications, China. He has published several books: "Introduction of EMC, Inductive Coupling and Resistive Coupling", as well as "Shielding and Grounding". He became an EMP Fellow of US Summa Foundation since 2010.